Article:
White, J.D., Ahrén, D., Ström, L. et al. (2023) Methane producing and oxidizing microorganisms display a high resilience to drought in a Swedish hemi-boreal mire. Journal of Geophysical Research: Biogeosciences, 128 (9). e2022JG007362. ISSN: 2169-8953

https://doi.org/10.1029/2022jg007362

JGR Biogeosciences

RESEARCH ARTICLE
10.1029/2022JG007362

Methane Producing and Oxidizing Microorganisms Display a High Resilience to Drought in a Swedish Hemi-Boreal Mire

J. D. White[1], D. Ahrén[2], L. Ström[1], J. Kelly[3], L. Klemedtsson[4], B. Keane[5], and F. J. W. Parmentier[1,6]

[1]Department of Physical Geography and Ecosystem Science, Lund University, Lund, Sweden, [2]National Bioinformatics Infrastructure Sweden (NBIS), Department of Biology, Lund University, Lund, Sweden, [3]Centre for Environmental and Climate Science, Lund University, Lund, Sweden, [4]Department of Earth Sciences, University of Gothenburg, Gothenburg, Sweden, [5]Department of Animal and Plant Sciences, The University of Sheffield, Sheffield, UK, [6]Centre for Biogeochemistry in the Anthropocene, Department of Geosciences, University of Oslo, Oslo, Norway

Abstract An increased frequency of droughts due to anthropogenic climate change can lead to considerable stress for soil microorganisms and their functioning within northern peatlands. A better understanding of the diversity and relative abundance of methane producing and oxidizing taxa, and their functional genes, can help predict the functional potential of peatlands and how the microorganisms respond to disturbances such as drought. To address knowledge gaps in the understanding of how functional genetic diversity shifts under drought conditions, we investigated a hemi boreal mire in Southern Sweden. Environmental parameters, including soil and air temperature, precipitation, and water table depth, as well as methane flux data were collected during the summer of 2017 under typical growing conditions, and in 2018 during a drought. In addition, the diversity and composition of genes encoding for methane metabolism were determined using the captured metagenomics technique. During drought we observed a substantial increase in air and soil temperature, reduced precipitation, and a lower water table depth. Taxonomic and functional gene composition significantly changed during the drought, while diversity indices, such as alpha and beta diversity, remained similar. These results indicate that methane producing and oxidizing microbial communities, and their functional genes, displayed a resilience to drought with specific genera having the ability to outcompete others under stress. Furthermore, our results show that although methane emissions are substantially reduced during drought, we can expect to see a shift toward more resilient methanogens and methanotrophs under future climate conditions.

Plain Language Summary Droughts and heat waves are increasing due to climate change. This can lead to considerable stress on soil microorganisms in northern wetlands which emit strong greenhouse gases such as methane. A better understanding of these methane producing and oxidizing microorganisms can help us predict how the community responds to droughts, and thus, how much greenhouse gases may be emitted in the future contributing further to climate change.

Key Points:

- Taxonomic and functional gene composition significantly changed during the drought
- Methane fluxes significantly reduced during drought but not in all ecotypes
- Specialist genera respond to drought stronger than others

Supporting Information:

Supporting Information may be found in the online version of this article.

Correspondence to:

J. D. White,
joel.white.2@gu.se

Citation:

White, J. D., Ahrén, D., Ström, L., Kelly, J., Klemedtsson, L., Keane, B., & Parmentier, F. J. W. (2023). Methane producing and oxidizing microorganisms display a high resilience to drought in a Swedish hemi-boreal mire. *Journal of Geophysical Research: Biogeosciences*, *128*, e2022JG007362. https://doi.org/10.1029/2022JG007362

Received 22 DEC 2022
Accepted 21 AUG 2023

Author Contributions:

Conceptualization: J. D. White, L. Ström
Data curation: J. D. White, B. Keane
Formal analysis: J. D. White, D. Ahrén, B. Keane, F. J. W. Parmentier
Funding acquisition: L. Ström
Investigation: J. D. White, F. J. W. Parmentier
Methodology: J. D. White, D. Ahrén, B. Keane, F. J. W. Parmentier
Project Administration: J. D. White, F. J. W. Parmentier
Resources: L. Klemedtsson
Supervision: D. Ahrén, L. Ström, L. Klemedtsson, F. J. W. Parmentier
Visualization: J. D. White, J. Kelly, F. J. W. Parmentier
Writing – original draft: J. D. White, F. J. W. Parmentier

1. Introduction

Anthropogenic climate change is one of the key issues of the twenty-first century, and it has the potential to severely impact natural peatlands through changes in temperature and precipitation (IPCC, 2021). While climate change models are forecasting increased precipitation at northern latitudes, these events are predicted to be more concentrated and less frequent in time with longer periods of dryer warm weather in between (IPCC, 2021). These events often result in a lowering of the water table depth which exposes methanogenic anaerobes to oxidative stress. This may decrease methane (CH_4) emissions to the atmosphere by reducing the habitable anoxic zone where methanogenic Archaea produce CH_4, but potentially also by increased activity and abundance of methanotrophs leading to a higher consumption of CH_4 (Keane et al., 2021; Rinne et al., 2020). These microbial communities inhabiting natural peatlands are vulnerable to disturbance under a warming climate, but potential structural shifts in microbial communities are currently difficult to predict, contributing to high uncertainties in current CH_4 budgets (Dean et al., 2018; Saunois et al., 2020).

Pristine peatlands function as long-term carbon sinks because plant productivity (CO_2 uptake) generally exceeds the slow rate of organic matter decomposition (CO_2 release) due to anaerobic conditions. Although these anaerobic conditions can lead to significant emissions of CH_4, over long-time scales, the carbon

Writing – review & editing: J. D. White, D. Ahrén, L. Ström, J. Kelly, L. Klemedtsson, B. Keane, F. J. W. Parmentier

balance of peatlands is primarily determined by the CO_2 fluxes (Rinne et al., 2020; Yu, 2012). However, the greenhouse gas balance of a peatland can shift from a sink to a source after drought, when expressed in CO_2-equivalents, due to the higher global warming potential of CH_4 (Fenner and Freeman, 2011; Rinne et al., 2020).

Drought conditions, that is, high air temperatures and reduced precipitation, result in a lower water table depth, aerating previously anoxic peat layers. This leads to increased heterotrophic respiration, and consequently a higher release of CO_2 to the atmosphere (Keane et al., 2021; Rinne et al., 2020). Concurrently, CH_4 emissions are reduced since oxygen (O_2) inhibits CH_4 production upon exposure to methanogen cells combined with increased methanotrophic CH_4 oxidization (Miller et al., 2019; Thauer et al., 2008). Due to these microbial controls, a deeper understanding of microbial structure and function, and the relationship to hydrological status, is required to improve projections of the role of peatland GHG emissions in the climate system.

Under anoxic conditions, inhibitory phenolic compounds can build up. These compounds are believed to reduce the activity of polyphenolic carbon degrading aerobes, that enable greater conversion of peat organic carbon into smaller substrates such as sugars, organic acids, H_2, and CO_2 that are more bioavailable for the anaerobic methanogens (Fenner and Freeman, 2011; Wilmoth et al., 2021). However, if O_2 is introduced through a drop in water table depth, phenol oxidase can remove phenolic inhibitors, enabling hydrolases to resume normal mineralization of organic matter that subsequently provide additional substrates for methanogenesis upon the return to anoxic conditions (Fenner and Freeman, 2011; Wilmoth et al., 2021). However, mounting evidence presented by Mcgivern et al. (2021) suggests that this process still occurs, but at a lower rate.

The taxonomic structure and function of methanogens is diverse and closely linked to hydrology status and warming (Bräuer et al., 2020). CH_4 production occurs stepwise in cooperation between different microbial functional groups, where organic carbon bound to dead organic matter is converted into CH_4 via methanogenesis (Dean et al., 2018; Ferry, 1999). Methanogenesis is a process catalyzed by specialized functional groups that convert CO_2 with H_2, methanol, methylamines, methylsulfides, or acetate into CH_4 (Thauer et al., 2008). Anaerobic methanogenesis is carried out exclusively by members of the archeal domain (Bräuer et al., 2020). Methanogens display high phylogenic diversity spanning three phyla (*Euryarchaeota*, *Halobacterota*, and *Thermoplasmatota*) and are no longer considered strict *Euryarchaeota* members. In total, five orders and two candidate taxa are commonly discovered in peat: *Methanomicrobiales*, *Methanocellales*, and *Methanosarcinales* of the phylum *Halobacterota*; *Methanobacteriales* of the phylum *Euryarchaeota*; *Methanomassiliicoccales* of the phylum *Thermoplasmatota*, and finally candidate family *Methanoflorentaceae* and candidate phylum *Bathyarchaeota* (Bräuer et al., 2020).

In contrast to methanogens, methanotrophs—of the phyla, *Proteobacteria*, *Verrucomicrobia*, and candidate phylum NC10—can oxidize CH_4 before it is emitted to the atmosphere, acting as a natural bio-filter. Aerobic methanotrophs belong to the Gammaproteobacteria (Type I, with families *Methylococcaceae* and *Methylothermaceae*), Alphaproteobacteria (Type II, with families *Methylocystaceae* and *Beijerinckiaceae*), and the Verrucomicrobia phyla (family *Methylacidiphilaceae*) (Guerrero-Cruz et al., 2021). Aerobic methanotrophs commonly inhabit the oxic-anoxic interfaces, where they oxidize between 10% and 90% of the CH_4 produced by methanogens (Hakobyan and Liesack, 2020; Wendlandt et al., 2010). Methanotrophs can be classified according to their taxonomy, carbon metabolism, morphology, and ecological life strategies (Guerrero-Cruz et al., 2021).

In this study, we focus on the drought that occurred during the summer of 2018 when Northwestern Europe, including Sweden, experienced a heatwave (Rinne et al., 2020; Sjökvist et al., 2019; Vicente-Serrano et al., 2010). Lower precipitation and higher temperatures altered the hydrological status of Swedish peatlands, leading to a lower water table depth, increased peat temperatures, and altered biogeochemical processes—including changes to methanogenesis. Although, methanogenesis is one of the most important carbon degradation pathways in peatlands (Keane et al., 2021; Kelly et al., 2021), knowledge on the resilience of methanogenic archaea to droughts in terms of community abundance, diversity and structure is still poorly understood and requires further attention (Kim et al., 2008).

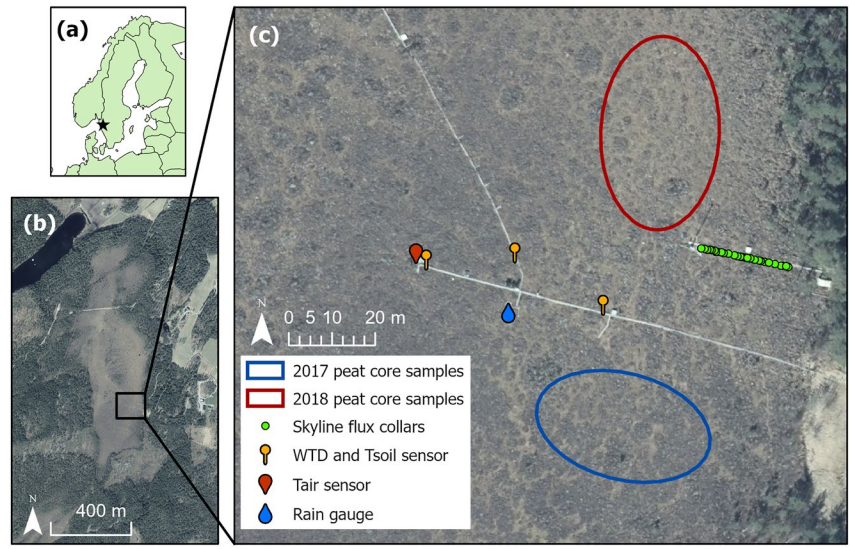

Figure 1. (a) Location of Mycklemossen (black star) within Sweden (b) aerial photo of Mycklemossen, black square shows the location of the sampling area and (c), map of peat core and ancillary measurement locations. Map data sources: © EuroGeographics and © Lantmäteriet.

Here, we address the functional potential of methanogenic and methanotrophic microbes in response to drought. We hypothesize that (a) the proportion of methanogenic and methanotrophic community shifts in relative abundance toward higher methanotrophic abundances when exposed to drought conditions. In addition, we aim to (b) determine which vegetative ecotype holds the highest microbial diversity during the drought, and (c), to identify whether the functional gene composition shifts in response to drought.

2. Materials and Methods

2.1. Site Description

This study focuses on Mycklemossen, a hemi-boreal mire dominated by bog-like vegetation, located in southern Sweden (58°21'N, 12°10'E). Mycklemossen is a sub-section of the Skogaryd Research Catchment and Swedish Infrastructure for Ecosystem Science network (https://www.fieldsites.se). Common to many hemi-boreal mires, the peatland consists of wet low areas dominated by *Sphagnum rubellum* and *Rhynchospora alba*, while the raised intermediate areas are a result of the tussock-building sedge *Eriophorum vaginatum*. Once the tussocks are established, the upper layers of the peat become drier and are no longer anoxic. This allows for the establishment of low shrubs such as *Calluna vulgaris*. The long-term (1990–2019) mean annual air temperature and total precipitation were 6.7°C and 1,021 mm respectively, as measured by the closest national monitoring station (Vänersborg, 10 km to the east and at a 30 m lower elevation than Mycklemossen).

2.2. Experimental Design

To determine the impact of the 2018 drought, we measured CH_4 fluxes, soil and air temperature, precipitation, water table depth, and collected peat samples for DNA-based analysis during 2017 and 2018. Measurements of CH_4 were made across a ~40 m long transect beginning at the tree line and extending into the mire. Plots were classified according to the dominant vegetation and are here represented as the *E. vaginatum* ($n = 6$), *C. vulgaris* ($n = 6$) and *R. alba* ($n = 6$) ecotypes. Replicate plots were identified at random and classified according to the dominant vegetation type. Peat samples for extraction of gDNA were removed from two different locations north and south of the boardwalk displayed in Figure 1. In 2017, 18 peat samples were collected from locations representing the *C. vulgaris* ($n = 6$), *E. vaginatum* ($n = 8$), and *R. alba* ($n = 4$) ecotypes south of the boardwalk

(Figure 1). In 2018, 11 samples were collected from *C. vulgaris* ($n = 2$), *E. vaginatum* ($n = 5$), *R. alba* ($n = 4$) ecotypes north of the boardwalk (Figure 1). Peat sampling was conducted in two similar sampling locations north and south of the boardwalk and these were separated by ∼60 m to avoid disturbance from previous sampling events (Figure 1). Both areas are similarly composed of hummocks and hollows and include equal representation of the pre-described ecotypes, which each exist within their own hydrological niche. The majority of the local peat deposits within the catchment extend down to 6 m depth (Wallin et al., 2015), with previous studies establishing no significant differences in surface or soil temperature between the hummocks and hollows (Kelly et al., 2021).

2.3. Environmental Variables

Meteorological variables were measured in both 2017 and 2018 with which we characterized the severity of the drought at Mycklemossen. Air temperature was measured with an HC2S3 sensor (Campbell Scientific, Logan, UT, USA) at 2 m above the peatland surface in a ventilated, radiation protected housing. Precipitation was measured with a tipping bucket rain gauge (SBS500H, Campbell Scientific, UK). Water table depth (CS450, Campbell Scientific, UT, USA) was measured at three different locations that represented the *C. vulgaris*, *E. vaginatum*, and *R. alba* ecotypes. The locations for soil and air temperature, precipitation and water table depth sensors are shown in Figure 1. All environmental variables were measured at 1 Hz and recorded on a CR1000 data logger (Campbell Scientific, UT, USA). Air temperature and water table depth values were averaged to represent daily means, while precipitation was summed to represent total daily values.

2.4. CH_4 Flux Measurements

Surface GHG fluxes were measured using the SkyLine2D system, an automated chamber system designed and built at the University of York For a full description of the SkyLine2D system, we refer to Keane et al. (2018). In short, the flux chamber comprised of a translucent Perplex cylindrical chamber (inner diameter 20 cm, height 40 cm), which was suspended from a motorized trolley and programmed to traverse ca. 2 m above the transect. The system was preset to visit the pre-selected plots along the transect, where the chamber was lowered onto pre-installed collars for a measurement period of 4 min. Following the 4-min measurement period, the system raised the chamber and moved to the next plot. The time taken to complete a full cycle was approximately 2.5 hr, which allowed each chamber to be measured ca. 10 times per day. The headspace gas from within the sealed chamber was circulated through a Los Gatos cavity ring-down laser (CRD, LGR U-GGA-91, Los Gatos Research, CA, USA) to measure the change in concentration of CH_4. Fluxes were calculated as the increase in headspace concentration over time, determined by linear regression, and adjusted for temperature and area of the chamber.

2.5. Captured Metagenomics

2.5.1. DNA Extraction

Peat material was collected using a 1.5 m long box corer from different locations within the mire that best represented the dominant vegetation ecotypes (Figure 1). Small samples of peat (∼30 g) were collected from the oxic-anoxic interface at ∼5 cm and within the anoxic zone, at ∼30 cm. Once separated from the cores, the peat material was immediately snap frozen using liquid nitrogen and stored in a −20°C freezer. Before DNA extraction was performed, samples were thawed for 4 hr in a refrigerator at 4°C. After thawing, gDNA was extracted from peat samples following the DNeasy® PowerSoil® Kit (Qiagen, Hilden, Germany) and carried out according to the manufacturers protocol, including the recommended 0.25 g of input material. Following the DNA extraction, samples were tested for quality (absorbance ratio 260/280) and concentration on a NanoDrop lite (NanoDrop Technologies, Wilmington, NC, USA) and Invitrogen Qubit 4 fluorometer (Thermo Fisher Scientific, Waltham, MA, USA), respectively.

2.5.2. SeqCap EZ Probe Generation

The metagenomic DNA extracted from the peat was processed to enrich for sequences of interest via the "captured metagenomics" method using oligonucleotide probes following White et al. (2022) and Manoharan et al. (2015). In short, genes that encode enzymes related to CH_4 production and consumption were identified from the Kyoto Encyclopedia of Genes and Genomes database (KEGG) (Kanehisa et al., 2015). In total, 548,104 sequences coding for methane metabolism were downloaded via a custom R script (https://github.com/dagahren/metagenomic-project) and compiled into a local database, subsequently called the CH_4 database. The nucleotide coding sequences of the CH_4 database were used to design custom hybridization-based probes for sequence capture according to Kushwaha et al. (2015). In total, 193,386 individual probes were generated after clustering, with a melting temperature of 55°C and probe length 40mer, suitable for use with the NimbleGen SeqCap EZ protocol (Roche NimbleGen Inc., Madison, USA).

2.5.3. Library Generation, Probe Hybridization and Sequencing

Depending on the concentration of the extracted DNA in a total volume of 100 µl low Tris-ethylenediaminetetraacetic acid buffer (TE), either 150 ng or 1 µg of gDNA was sheared using a Bioruptor Pico in 0.65 ml Bioruptor tubes for 13 cycles—30s on, 30s off (Diagenode SA, Seraing, Belgium). The fragmented DNA was purified using 1.8× AMPure XP beads (Beckman Coulter) and used as input material for preparation of pre-capture libraries. Libraries were constructed according to the Nimblegen SeqCap EZ HyperCap Workflow User's Guide (Version 1.0 June 2016) with the following modifications: (a) for the adapter ligation step, 5 µl of 15 µM KAPA unique dual index mixed adapters were used instead of single index adapters, (b) for the pre-capture PCR, 7 cycles were used for libraries with a genomic DNA input of 150 ng, and 5 cycles where the input was 1 µg.

Libraries were multiplexed in pools of 15 in equimolar amounts based on the concentrations and sizes. 1 µg of each pool was transferred to a test tube and hybridized to the custom probes according to the NimbleGen SeqCap EZ SR User's Guide (Version 4.3 October 2014). The capture tubes were incubated in a thermal cycler set at 47°C, heated lid set to 57°C for 69 hr. The quantity and quality of the final pool was assessed by Qubit and Bioanalyzer and subsequently by qPCR using the Illumina Library Quantification Kit from Kapa on a Roche Light Cycler (LC480II, Basel, Switzerland).

The captured libraries were sequenced on an Illumina HiSeq4000 platform using sequencing by synthesis technology to generate 2 × 150 base paired end reads. The analysis was carried out at the Center for Genomic Research, University of Liverpool, UK.

2.6. Data Processing and Statistics

2.6.1. Environmental Variables

All environmental data, including soil and air temperatures, precipitation and water table depths were measured daily from the 1st of May to the 30th of September, which we refer to as the growing season. To identify the differences in means between the environmental variables, we used a non-parametric Wilcox-ranked sum test via the R base package (R Core Team, 2022) to identify differences in the means of air temperature, soil temperature and water table depth, according to the defined ecotypes and between 2017 and 2018.

2.6.2. CH_4 Flux

CH_4 flux data was quality controlled by discarding measurements with a R^2 value ≤ 0.9. Measurements passing this threshold were then assessed using the output statistics from the regression calculation, where regressions with a p value ≤ 0.05 were accepted, while those that did not were treated as zero flux. To allow for the temporal and repeated measures data, differences in CH_4 fluxes between years and ecotypes were tested using linear mixed effects models via the lme4 package v1.1–27.1 (Bates et al., 2015). CH_4 flux was set as fixed effect within the model while ecotype and year were random. Differences were calculated using estimated marginal means in combination with a Tukey pairwise post-hoc tests on significant effects.

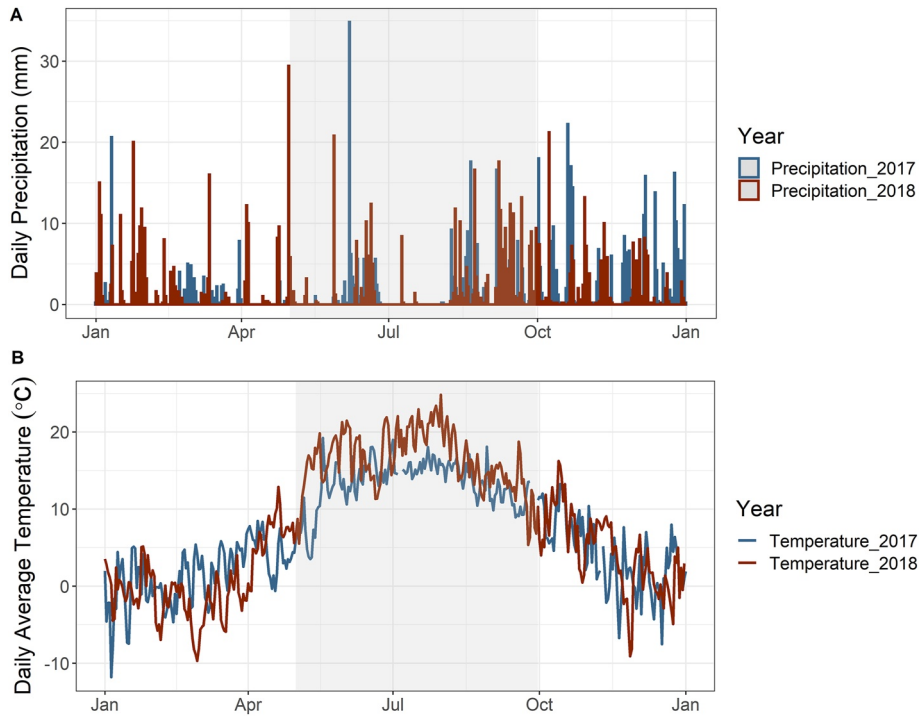

Figure 2. (a) Daily mean temperature measured in °C and (b) Daily summed precipitation measured in millimeters at Mycklemossen mire. 2017 is shown in blue and 2018 in red. The shaded area indicates the growing season from May 1st to September 30th.

2.6.3. Sequence Annotation

Raw sequencing files were trimmed for the presence of Illumina adapter sequences using the software package Cutadapt v1.2.1 (Martin, 2011). The reads were further trimmed using Sickle v1.2 with a minimum window quality score of 20 (Joshi and Fass, 2011). Following trimming, reads shorter than 20bp were discarded. The sequence reads from each of these captured data sets were processed through MG-RAST, an online metagenomics annotation program (Meyer et al., 2008). Further detail regarding the annotation pipeline can be found in Supporting Information S1 and in Meyer et al. (2008).

Following the MG-RAST pipeline, annotated sequences were further filtered for both taxonomic and functional annotations using the KEGG methane metabolism filter (KO:00680). The filter includes both taxonomic and functional related to CH_4 metabolism and excludes remaining off target sequences. Sequence data and functional annotations are freely available through MG-RAST with the accession ID mgp91145.

2.6.4. Taxonomic Diversity and Functional Genes

All analyses of taxonomy and function genes were calculated in R studio v 3.6.1 (R Core Team, 2022) using the vegan package v2.5 (Oksanen et al., 2019) and visualized via the ggplot2 package v 3.3.2 (Villanueva and Chen, 2019). Alpha diversity was calculated using the Shannon-Weiner Species Diversity Index by taking the number of each species, the proportion each species represents of the total number of individuals, and sums the proportion times the natural log of the proportion for each species. Beta diversity was calculated using Bray-Curtis distances to quantify categorical variation in the overall taxonomic composition between ecotypes. To identify significant differences between year and ecotypes for taxonomic and gene abundances a PERMANOVA was chosen (Anderson, 2001). Due to the small sample sizes and uneven distribution of replicates, we normalized taxonomic and functional gene abundances via a double square root transformation. This allowed for highly abundant taxonomic and functional gene counts, zeros within the data matrix and

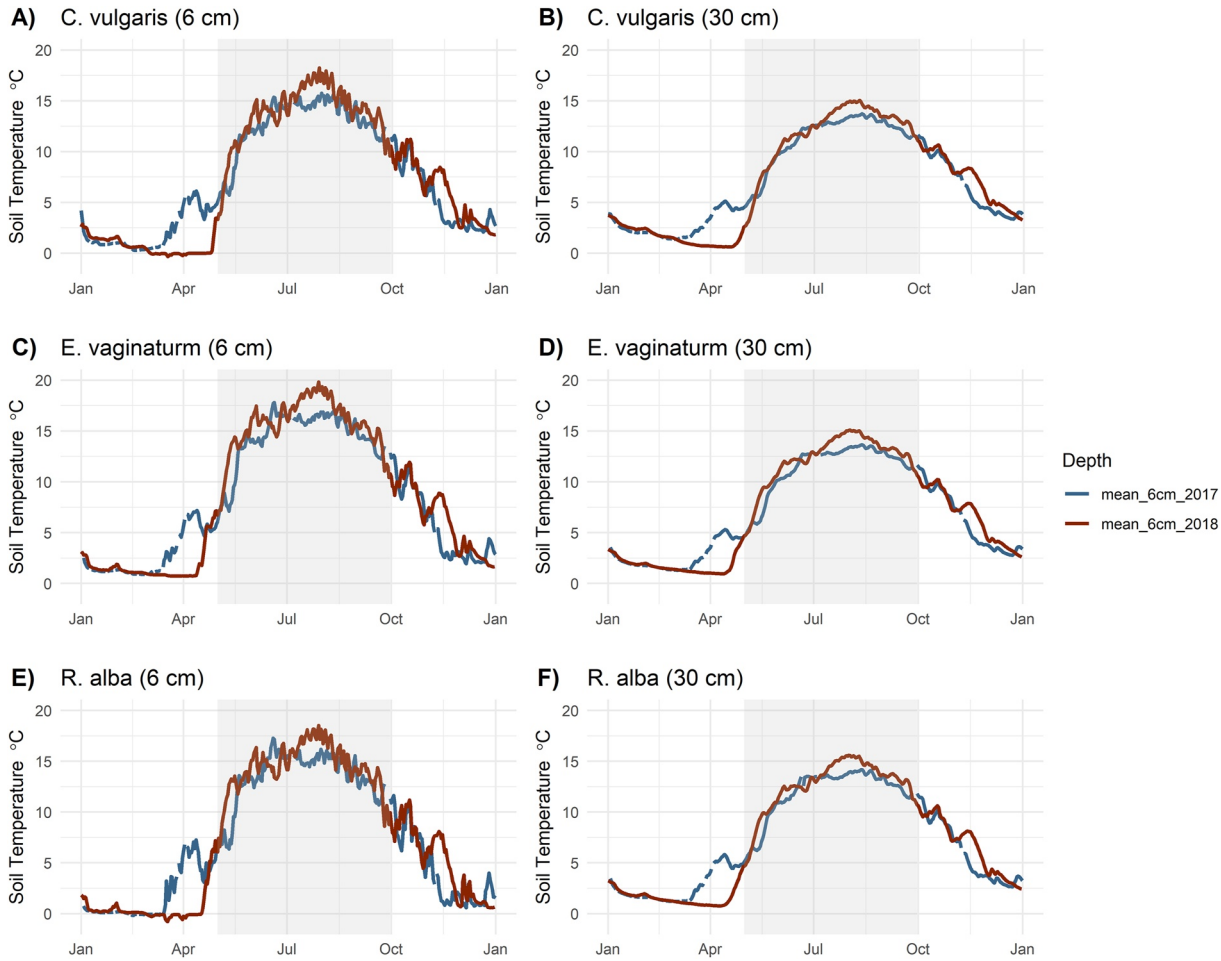

Figure 3. Daily mean soil temperature measured at 6 and 30 cm below the peat surface. Blue lines indicate 2017 values while red lines indicate 2018 values. The shaded area indicates the growing season from May 1st to September 30th.

uneven sequencing depth (Weiss et al., 2017). This gives the best representation of biological variation rather than sequencing variation. Following transformation, we calculated ordination for NMDS and PCoA plots using Bray-Curtis distances and a Wilkson pairwise post-hoc test was used to identify significant differences between ecotypes and years. Finally, a SIMPER analysis was performed through pairwise comparisons of groups of sampling units to find the average contributions of each species to the average overall Bray-Curtis dissimilarity.

3. Results

3.1. Environmental Variables

In 2018, Mycklemossen mire experienced a maximum air temperature of 33°C that was reached on the 31st of July 2018 (Figure 2a). Daily mean air temperature during May-September reached a maximum of 24.8°C (SD ± 3.95) in 2018, a 5.6°C increase in comparison to 2017. On average, all daily mean soil temperatures during the growing season were higher in 2018 when compared to 2017. The high air temperature was also reflected in the soil temperature, where the maximum daily values in August 2018 were 3.4°C higher at 6 cm depth and 1.3°C higher at 30 cm depth in the *C. vulgaris* ecotype compared to 2017 values (Figures 3a and 3b). The *E. vaginatum* ecotype followed the same pattern with 2°C higher at 6 cm depth and 1.5°C higher at 30 cm depth (Figures 3c

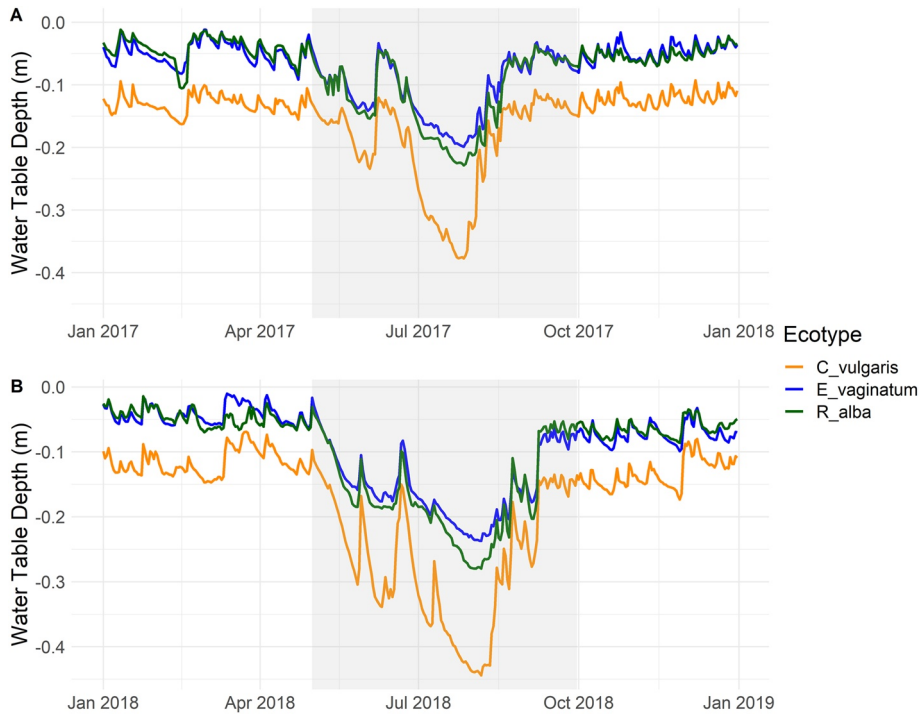

Figure 4. Water table depth in meters below the surface for *C. vulgaris*, *E. vaginatum* and *R. alba* ecotypes from automated sensors at the site during 2017 (a) and 2018 (b). The shaded area indicates the growing season from May 1st and September 30th.

and 3d). The final ecotype, *R. alba,* had a slightly lower deviation with 1.4°C higher at 6 cm depth and 1.2°C higher at 30 cm depth (Figures 3e and 3f).

Daily summed precipitation values in 2018 were below average during the growing season from May to October (Figure 2b), with predominantly dry conditions in July 2018 when only 10.2 mm of rain was recorded, compared to the long-term average of 80 mm. Significantly lower rainfall was observed in 2018 during the whole growing season when compared to 2017 values ($p \leq 0.04$) (Figure 3). This decrease in precipitation resulted in a lower water table depth across the whole peatland (Figure 4). Significantly lower WTD's were observed in both *E. vaginatum* ($p \leq 0.02$) and *R. alba* ($p \leq 0.02$), resulting in a lower water table depth up to 4 and 9 cm in 2018 (Figure 4b*).* In the *C. vulgaris* ecotype, the water table dropped by as much as 7 cm in 2018 when compared to 2017.

3.2. Methane Fluxes

The highest daily mean CH_4 fluxes (33.3 CH_4 nmol m^{-2} s^{-1}) were observed during the growing season in 2017, significantly higher than in 2018 (25.7 CH_4 nmol m^{-2} s^{-1}) ($p \leq 0.001$). The ecotype that yielded the highest mean CH_4 flux was *R. alba* in 2017 with a mean flux of 48.1 CH_4 nmol m^{-2} s^{-1} (SD ± 3.11) followed by *E. vaginatum* (34.1 SD ± 6.36 CH_4 nmol m^{-2} s^{-1}) and *C. vulgaris* (17.8 SD ± 2.58 CH_4 nmol m^{-2} s^{-1}). During the drought in 2018, fluxes in the *R. alba* ecotype significantly reduced by 29% ($p \leq 0.0001$), and by 27% ($p \leq 0.04$) in the *C. vulgaris* ecotype, while the smallest reduction was observed in *E. vaginatum* (10%) ($p \geq 0.05$) (Figure 5).

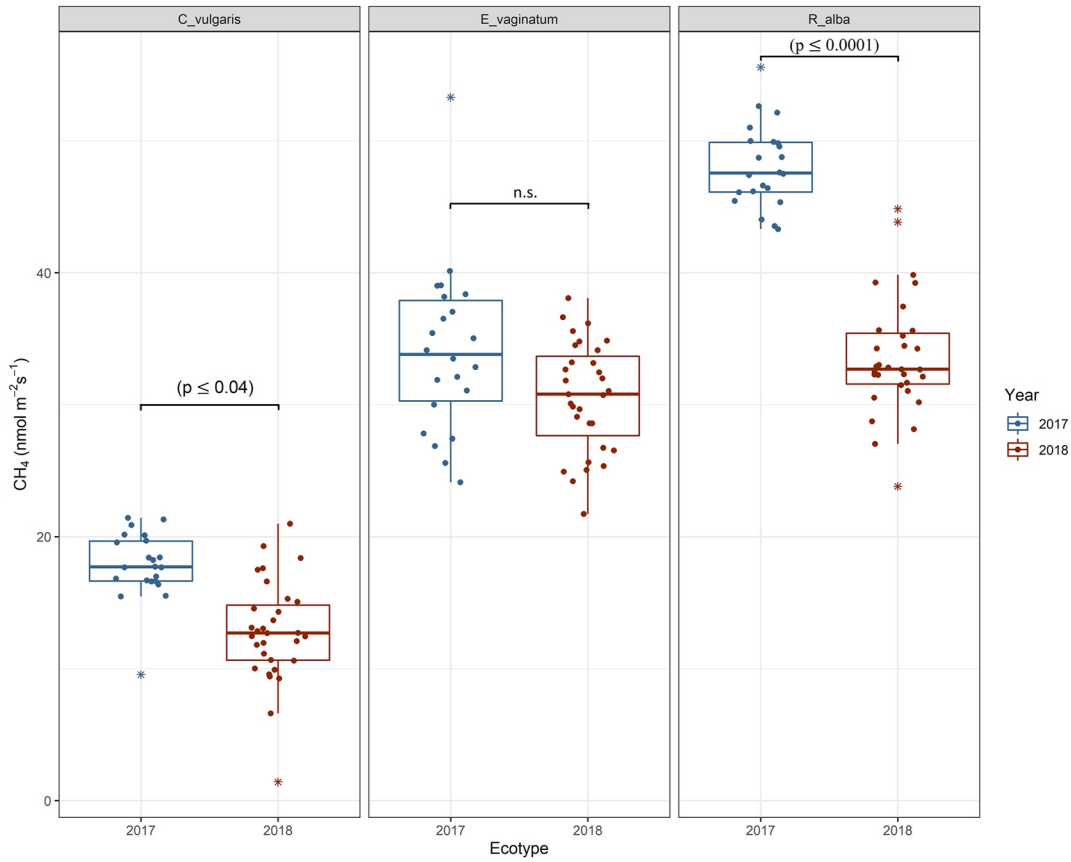

Figure 5. Boxplots of daily mean CH_4 flux measured during the growing season (May to October) in 2017 (blue) and 2018 (red) at Mycklemossen mire. The boxes show quartiles and the median, the whiskers denote data within 1.5 times of the interquartile range. Colored stars denote outliers while significant differences using linear mixed effects models are labeled with the *p* value and "n.s." indicates a non-significant result.

3.3. Taxonomy

3.3.1. Taxonomy Overview

At the genus level, 20 methanogenic genera were identified. The highest abundant methanogens included *Methanoregula*, *Methanosarcina*, and *Methanosphaerula*. Within the methanogen community, genera with the ability to metabolize via hydrogenotrophic, acetoclastic, and methylotrophic methanogenesis pathways were all detected. While within the methanotroph community, five genera of methanotrophs were also identified. Methylocella held the highest relative abundance, followed closely by Methylosinus and Methylococcus. As observed in the methanogen community, methanotrophs with the ability to metabolize via the serine and the ribulose monophosphate pathway were also present.

3.3.2. Proportions of Methanogens to Methanotrophs Between Years

Large significant variations in the relative abundances of methanogens and methanotrophs were observed between drought and non-drought years, with 36% of the variation explained by the year ($R^2 = 0.36$, $p \leq 0.003$) (Figure 6a). Clear clusters can be observed in Figure 6a with only a small overlap in samples. A mantel test was used to determine whether there was a correlation between distance and Bray-Curtis dissimilarity matrices with the corresponding GPS positions. We found that the Bray-Curtis dissimilarity matrix did not have a significant relationship with the geographic separation of the samples (Mantel statistic R: 0.1474, p value = 0.1194). Therefore, as samples became physically more separated their corresponding microbial communities didn't necessarily become more dissimilar. This points toward a response to drought rather than it being due to spatial variability.

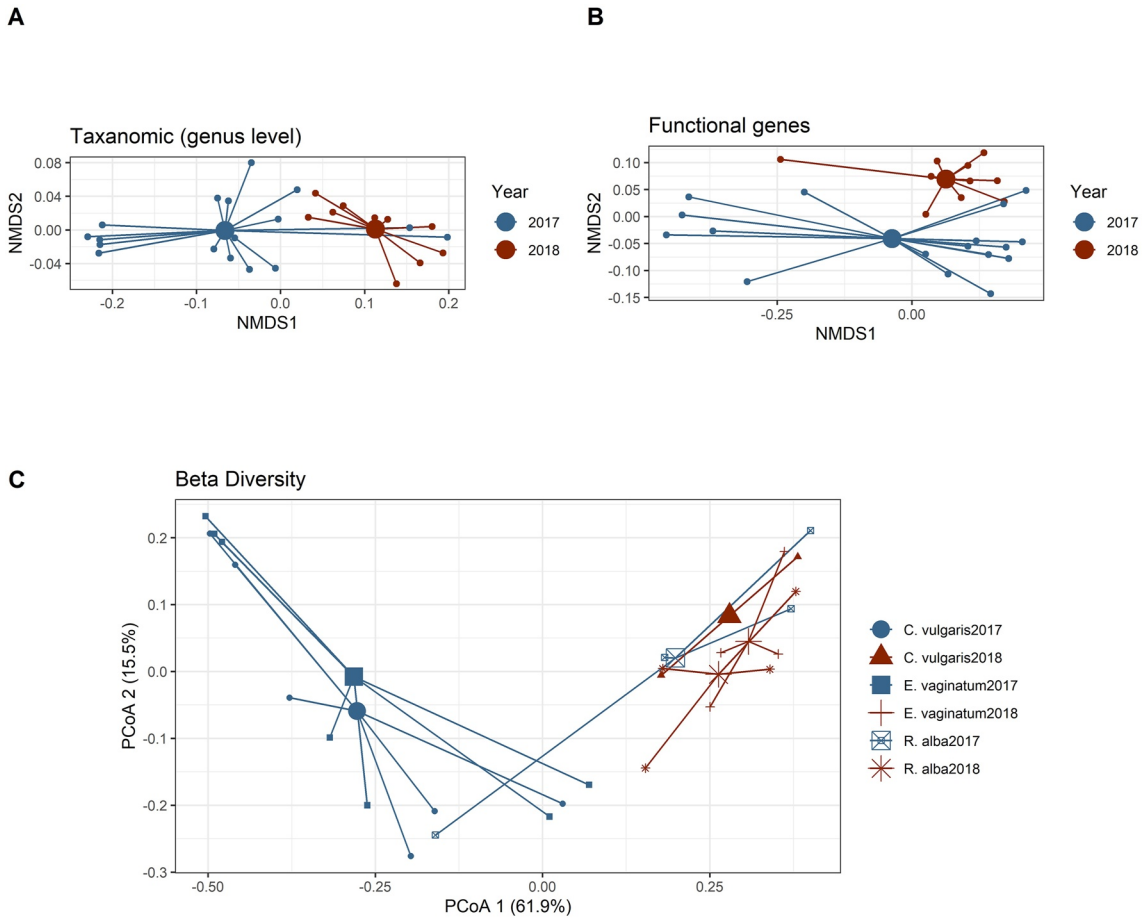

Figure 6. (a) Non-metric Multidimensional Scaling (NMDS) of taxonomic abundances using Bray-Curtis distances. Small dots indicate individual samples while the largest dots indicate the mean of all samples. Samples were analyzed at genus level and colored by year 2017 ($n = 17$) and 2018 ($n = 10$). (b) Nonmetric Multidimensional Scaling (NMDS) of functional genes using Bray-Curtis distances. Small dots indicate individual samples while the largest dots indicate the mean of all samples. Samples were analyzed at KO level 4 and colored by year 2017 ($n = 17$) and 2018 ($n = 10$). (c) Principal Coordinates Analysis (PCoA) of taxonomic abundances using Bray-Curtis distances. Small symbols indicate individual samples while the largest symbols indicate the mean of all samples. Samples were analyzed at genus level and colored by ecotype and sampling year (*C. vulgaris* 2017 ($n = 6$) 2018 ($n = 2$), *E. vaginatum* 2017 ($n = 7$) 2018 ($n = 4$), *R. alba* 2017 ($n = 4$) 2018 ($n = 4$).

The average proportion of methanogens to methanotrophs during 2017 was 59% and 41% respectively. In 2018, however, the proportion of methanogens decreased by 8%, while the proportion of methanotrophs increased to 49%. The genus which contributed the most to dissimilarity according to the SIMPER analysis—that calculates the contribution of each species (%) to the dissimilarity between each group—was *Methylocella,* with an 0.12 average contribution to the overall dissimilarity (Table 1). The average relative abundance for *Methylocella* significantly increased by 219% during the drought in 2018 when compared to 2017 ($p \leq 0.001$). Interestingly, the average relative abundance of all methanogens and methanotrophs increased during the drought, with *Methanoregula* contributing the highest to dissimilarity, followed by *Methanosarcina*. In addition, all detected methanotrophs significantly increased, including the type I, II and *Verrucomicrobia* when tested between years ($p \leq 0.005$).

3.3.3. Ecotype Comparison

A large dissimilarity in the relative abundance of taxa was observed when comparing ecotypes between each year. This variation in taxonomic relative abundance resulted in a significant correlation where 58% of the variation in taxonomic relative abundance could be explained by ecotype ($R^2 = 0.58$, $p \leq 0.002$). The Wilks pairwise test indicated that significant dissimilarity occurred for *E. vaginatum* between 2017 and 2018 ($p \leq 0.03$), but the same dissimilarity was not observed for *R. alba* and *C. vulgaris* ($p \geq 0.05$).

Table 1
Results of Taxonomic Contribution of Each Species (%) to the Dissimilarity Between Each Group (SIMPER Analysis) Between 2017 and 2018

Genus	Average contribution to dissimilarity	SD	Avg. 2017	Avg. 2018	Percentage contribution	p-value
Methylocella	0.12	0.089	2,539	8,108	20%	0.001
Methanoregula	0.09	0.085	4,267	5,968	36%	1
Methylosinus	0.08	0.050	2,386	5,602	49%	0.031
Methanosarcina	0.05	0.032	1,529	4,142	58%	0.006
Methylococcus	0.03	0.022	814	2,495	64%	0.001
Methylacidiphilum	0.03	0.020	568	1,935	69%	0.001

Note. Taxa are ranked according to their average contribution to dissimilarity between years. Average relative abundances, percentage of cumulative contribution and Permutation *p*-value (Probability of getting a larger or equal average contribution in random permutation of the group factor) are also included. A cut-off at a cumulative dissimilarity of 70% was applied (2017 $n = 17$: 2018 $n = 10$).

When comparing the relative abundance of methanogens and methanotrophs between *E. vaginatum*, *R. alba*, and *C. vulgaris*, six genera were the most common within the top 70% of cumulative sums, irrespective of ecotype: *Methanoregula*, *Methylocella*, *Methylosinus*, *Methanosarcina*, *Methylococcus*, and *Methylacidiphilum* (Table S1, S2 and S3 in Supporting Information S1). *Methanocaldococcus and Methanosphaerula* were within the top 70% of cumulative sums for the *R. alba* ecotype (Table S2 in Supporting Information S1), but not *E. vaginatum* (Table S1 in Supporting Information S1) or *C. vulgaris* (Table S3 in Supporting Information S1).

When comparing *R. alba* and *C. vulgaris,* we observe that the hydrogenotrophic *Methanoregula* contributed the most to dissimilarity (Table S2 and S3 in Supporting Information S1). Although type II *Alphaproteobacteria genera*, *Methylocella*, and *Methylosinus* were the second and third most important among ecotypes, the order of dissimilarity of *Methylocella* and *Methylosinus* changed according to ecotype. Within the *E. vaginatum* comparison, the dominant *Methanoregula* was surpassed by *Methanosarcina*, with an average dissimilarity of 0.07, when compared to the remaining ecotypes.

3.4. Functional Gene Composition

The functional genes showed a clear separation between 2017 and 2018, with only a small overlap between clusters (Figure 6b). The largest variation of functional genes occurred in 2017, with smaller variation observed in 2018. Significant differences were observed between the relative abundance of functional genes when tested via PERMANOVA between 2017 and 2018 ($p \leq 0.036$). In addition, the PERMANOVA revealed that 12% of the variance in relative abundance can be explained by the year ($R^2 = 0.12$, $p \leq 0.036$).

In total, 106 functional genes related to CH_4 metabolism were captured, with 20 contributing to the top 70% cumulative sum of dissimilarity between CH_4 functional genes (Table S4 in Supporting Information S1). Within the top 70% cumulative contributions, 12 out of the 20 captured genes saw an increase in average relative abundance during 2018. The gene contributing most to the dissimilarity was heterodisulfide reductase subunit A (*hdrA*). The *hdrA* gene held an average relative abundance of 627 in 2017, resulting in an 86% increase in 2018 ($p \geq 0.05$). Genes including *cutL*, *hdr*, *fdhA*, *coxS*, *frmB*, *mvhA*, *metF*, and *cutM* were all significantly more abundant in 2018 when compared to 2017 values ($p \leq 0.05$). Genes that did not increase during 2018 included *frhA*, *mcrA*, *frhG*, *hdrB*, *fwdB*, *mtd*, *mtrE*, *and mtrH*.

4. Discussion

In this study, we observed the effect of drought on the functional potential of CH_4 producing and oxidizing microorganisms. In general, methanogens and methanotrophs displayed a high resilience to drought conditions, with shifts in proportion toward more methanotrophs during drought. In addition, the relative abundance of both methanogens and methanotrophs increased with the largest increase in observed within genera with expanded genomic features that enable better tolerance toward oxidative environments that is, *Methanosarcina*.

4.1. Structural Shifts in Response to Drought

CH_4 emissions from peatlands have been largely attributed to the metabolism of methanogens, balanced by oxidation via methanotrophs (Dean et al., 2018). Here, we hypothesized that the proportion of methanogenic community shifts toward higher relative methanotrophic abundance when exposed to drought conditions. This hypothesis was confirmed when we observed an increase of 8% in the relative abundance of methanotrophs during drought conditions. This shift was also reflected in the CH_4 flux, where both *C. vulgaris* and *R. alba* ecotypes had significantly lower fluxes during the drought. However, in the *E. vaginatum* ecotype, a significant reduction was not observed, despite showing the same trend as the other ecotypes. Further quantitative methods such as qPCR of the *mcrA* or *pmoA* gene would be needed to confirm if this observed reduction was a result of increased production or oxidation as observed in Zhang et al. (2022). We hypothesize that the drop in water table led to increased O_2 availability, phenol oxidase activity and higher peat temperatures. This shift in favorable conditions within the peat profile provided a much better habitat to increase methanotroph abundance, which were previously held lower due to the unfavorable conditions and presence of phenolic compounds. This result is in agreement with findings from Amodeo et al. (2018), where the authors reported that the optimum growth for methanotrophs is between 20°C and 25°C combined with a 1:1 ratio of CH_4:O_2. Therefore, favorable conditions, that is, increased peat temperature, O_2 availability and CH_4 originating from deeper anoxic layers may have led to an increase of the methanotroph community during the drought (Table 1, Tables S1–S4 in Supporting Information S1).

The three main methanotrophs driving the increased proportion under the drought were type II: *Methylocella*, *Methylosinus* and type I: *Methylococcus*. Type II genus *Methylocella* and *Methylosinus* contributed the highest to the total microbial sum, which was also observed in previous studies (Ho et al., 2011). Ho et al. (2011) observed the same pattern of rapid initial growth of type II methanotrophs in severely disturbed microcosms from rice paddies, whereas growth of type I methanotrophs were stunted. Although type I methanotrophs were not stunted in our results (i.e., *Methylococcus*), type II methanotrophs increased more in proportion when compared to type I, indicating that type II methanotrophs may be better adapted to drought conditions and are not limited by their main substrates CH_4 and O_2 and other nutrients, but rather, the amount of habitable zone within the peat column.

Interestingly, the relative abundance of both methanogens and methanotrophs increase during drought. Several studies concluded that methanogenesis is suppressed upon exposure to O_2 (Ma et al., 2012; Yuan et al., 2009), while we observed a reduction in CH_4 flux but not a total cessation of CH_4 emissions. The same was observed by Rinne et al. (2020) and similar results have been observed in flooded paddies, lake sediments and bromeliad tanks where members belonging to *Methanocellaceae* and *Methanosarcinaceae* increase in relative abundance following desiccation (Brandt et al., 2015; Conrad et al., 2014). One explanation to the increase in abundance may be explained by methanogens including *Methanoregula*, *Methanosarcina*, and *Methanosphaerula* that possess expanded genomic features including the ability to deal with O_2 stress, thus, a better adaptation to oxidative environments (Lyu and Lu, 2018). In this study, the relative abundance of the dominant methanogen, the hydrogenotrophic *Methanoregula*, remained unchanged during both drought and non-drought conditions, neither decreasing nor increasing significantly. However, the most metabolically versatile of the methanogens, *Methanosarcina*, increased significantly under drought conditions within the ecotype *E. vaginatum*, presumably due to the presence of oxygen-detoxifying enzymes such as catalase, superoxide dismutase, and superoxide reductase that give this methanogen a particular eco-physiological advantage that allows for growth during desiccation (Angel et al., 2011; Conrad et al., 2014; Erkel et al., 2006). Therefore, we propose that the physiological characteristics of the community indicate that both hydrogenotrophic and acetoclastic methanogens, especially facultative methanogen (i.e., any organism that can grow either with or without free oxygen) members belonging to the class *Methanosarcinales*, are more resilient to drought conditions and O_2 exposure than other genera observed here.

Methanogenesis and microbial growth are temperature dependent processes (Van Hulzen et al., 1999). Although methanogenesis can be inhibited when exposed to O_2, our flux measurements show that not all methanogenesis stopped. It is possible that, following the drop in water table, not all water evaporated, resulting in peat macropores acting as anoxic microbial refuges. It is also possible that microscale anoxic sites were formed within soil aggregates, which provide an ecological refuges for the survival of methanogens exposed to O_2 stress (Yuan et al., 2009). These ecological refuges still hold the necessary environmental conditions for methanogenesis to occur, but with an increased temperature that can increase metabolic activity.

Incubation studies by Van Hulzen et al. (1999) found that alternative electron acceptor reduction increases with a rise in temperature, indicating that available electron acceptors will be reduced sooner—resulting less competition to

methanogen growth. When all alternative electron acceptors are consumed, the population size of the methanogens is the limiting factor in CH_4 production. Therefore, we believe that the increased soil temperature coupled with the eco-physical advantage demonstrated by multiple functional groups may explain the increased relative abundance of methanogens during the drought, which is consistent with other studies (Brandt et al., 2015; Conrad et al., 2014).

During drought and the lowering of the water table, the relative abundance of aerobic methanotrophs increased significantly. Previously uninhabitable anoxic environments within the peat column became aerobic, allowing a competitive edge for genera such as *Methylocella* and *Methylosinus*, which are strict aerobes. Previous studies have reported increased methanotroph relative abundance associated with higher magnitudes of CH_4 flux (Van Hulzen et al., 1999; White et al., 2022), however the same results are not observed here, indicating that the reduction in CH_4 flux may be caused by an increase in methanotrophy. *Methylocella*, a facultative methanotroph, was the dominant methanotroph in all ecotypes. This trend may be explained by the capability of *Methylocella* growing on CH_4 as well as multicarbon substrates (Dedysh and Dunfield, 2011). This means that under stressful conditions such as drought, *Methylocella* can metabolize via multiple alternative metabolic pathways, yielding a competitive advantage over other obligate methanotrophs. These results were also observed in Ho et al. (2015) and Ma et al. (2012), where they showed that the recovery of type I methanotrophs needed more time between drying events. Therefore, during a drought we expect type II methanotrophs to dominate. Our results indicate that methanotrophs are highly resilient to droughts, but their resilience may still reach a "critical point" where activity is no longer recovered if droughts persist on longer time scales and increase in frequency.

4.2. Taxonomic Diversity Between Ecotypes

During the drought, the overall diversity of methanogens and methanotrophs did not change. We observed small non-significant variation in the means of α-diversity between drought and the control year. These findings are in line with results from Kim et al. (2017), where there were no differences in the diversity and composition of the microbial communities between control and a 4-week drought. In contrast, Zhong et al. (2017) showed significant difference in observed species and Shannon α-diversity of prokaryotic microbiota following water table draw down. However, these results were based on a 46-year time interval where the original peatland was drained for livestock grazing. These results suggest the need to research the effects of repetitive and long-term disturbance from drought in the future. Therefore, we observe that the resilience of methanogens and methanotrophs to the effects of drought is high under short periods of time, but more research is needed on the effects on community structure and function during sustained droughts.

4.3. Effect of Ecotype on CH_4 Fluxes

During the drought, significantly lower CH_4 fluxes were observed in *C. vulgaris* and *R. alba* ecotypes, but not in *E. vaginatum*, although a similar trend was detected. We believe that the presence of aerenchyma tissue within the sedge *E. vaginatum* tillers, plus the ability for the sedge species to access anoxic layers through deep roots, allowed access to CH_4 produced in deeper anoxic layers. This physiological trait facilitates the transport of CH_4 produced in deep anoxic peat layers directly to the atmosphere, by-passing aerobic upper layers where methanotrophy can oxidize CH_4. Our results are consistent with previous studies conducted in peatlands where vegetative cover is directly related to the magnitude of CH_4 flux (Keane et al., 2021; Korrensalo et al., 2018).

The ecotype with the largest reduction in CH_4 emissions during the 2018 drought was *R. alba*. This ecotype is usually dominated by high water table depths and sphagnum mosses, indicative of conditions favoring CH_4 production. Interestingly, previous studies conducted across the globe have identified moss-associated methane oxidizers inhabiting *Sphagnum* (Kip et al., 2010), and revealed that moss-associated methane oxidizers can exceed methanogenic activity in terrestrial sites by up to two orders of magnitude (Liebner et al., 2011), but this relationship was not observed in our results. One possible explanation is the presence of *R. alba*, a sedge species with aerenchyma tissue similar to *E. vaginatum*. However, the rooting length of *R. alba* is substantially shallower than *E. vaginatum*, resulting in limited access to deep anoxic layers. Thus, we do not observe the same by-passing of aerobic upper layers where methanotrophs can oxidize CH_4, therefore reducing net CH_4 emissions.

Finally, the *C. vulgaris* ecotype had the lowest CH_4 emissions in both 2017 and 2018, consistent with previous studies (Keane et al., 2021). *C. vulgaris* dominated the drier portion of the bog, where it is expected to see a combination of low methanogenesis and high methanotrophy, due to the aerobic conditions and lack of plant mediated CH_4 transport through sedges.

4.4. Functional Genes During Drought

Our results indicate that the structure and relative abundance of functional genes related to CH_4 metabolism significantly change when exposed to drought conditions. 12% of the variance in relative abundances were explained by year, with the highest variation in functional gene relative abundance observed under non-drought conditions. One possible explanation is that droughts increase the abundance of genera with greater genetic capacities to survive drought conditions, since these individuals can take better advantage of the aerobic conditions that may inhibit metabolic activity in other genera.

The top three genes that contributed the most to the dissimilarity during the drought were *hdrA,* carbon monoxide dehydrogenase large subunit (*cutL*) and hydrogen dehydrogenase. The *hdrA,* combined with methyl-coenzyme M (*mcrA*), functions together in the biological formation of CH_4. *mcrA* catalyzes the conversion of methyl-coenzyme M and coenzyme B into CH_4 and the heterodisulfide of coenzyme M (HS-CoM) and coenzyme B (HS-CoB) (Scheller et al., 2010; Thauer, 2019). Subsequently, CoM and CoB must be reduced to regenerate the CoM-SH and CoB-SH thiols that are used as electron donors by *mcrA,* which is then catalyzed by *hdrA* (Buan et al., 2011; Scheller et al., 2010). White et al. (2022) observed a co-dependence between *mcrA* and *hdrA,* indicating the close nature of the two genes for the biological formation of CH_4. Here we observe increases in the relative abundance of *hdrA*—but not *mcrA* –potentially resulting in a reduction in the conversion of *mcrA* and coenzyme B into CH_4. The lower fluxes suggest this, but it is challenging to determine whether the relative abundances of *hdrA* come exclusively from methanogens, as *hdrA* is a common gene shared between multiple microbial groups including *Acetogens,* sulfur oxidizing *Archaea* and *Bacteria* (Ernst et al., 2021). Therefore, it is difficult to determine whether the increase is related to methanogens or other microbial communities. In addition, we observed significant increases in the relative abundance of carbon monoxide dehydrogenase genes (*cutL*, *coxL*, *coxS* and *cutM*) under drought conditions. According to Ferry (2010), it is not yet known if carbon monoxide is a viable energy source for methanogens in peatland environments. The association between methanogenesis and the Acetyl-CoA pathway appears to be much more flexible than previously thought (Borrel et al., 2016). Finally, it must be noted that the relative abundance of functional genes is not an ideal proxy for linking microbial activity to CH_4 fluxes. The analysis of expressed gene transcripts via a metatranscriptomics or qPCR approach would be a more suitable method for drawing such conclusions.

4.5. Taxonomic Diversity

In 2017, the mean α-diversity was 2.30 (±0.24), while in 2018 the mean α-diversity was 2.49 (±0.25), but this is a non-significant difference. Between ecotypes, diversity was determined with the β-diversity index (Figure 6c). During 2017, the highest mean distance of group members to the group centroid was observed in *R. alba* plots (0.36 ± 0.26) followed by *E. vaginatum* (0.33 ± 0.11) and *C. vulgaris* (0.33 ± 0.13). In 2018, this order was not observed and the *C. vulgaris* ecotype had the highest mean β-diversity (0.36 ± 0.0), followed by *R. alba (0.25* ± 0.09) and *E. vaginatum* (0.17 ± 0.09). Although we see small shifts between ecotypes and years, the ANOVA's *p*-value is not significant, meaning that group dispersions are homogenous ($p \geq 0.05$).

5. Conclusions

Our study provides in situ evidence on how drought affects the functional potential of microorganisms responsible for CH_4 production and oxidation in hemi-boreal peatlands. The functional potential during the drought differed significantly when compared to the previous year. In response to the drought, the proportion of methanogens to methanotrophs shifted in favor of more methanotrophs, driven by the facultative *Methylocella*. Our results suggest that (I) specific functional groups respond differently to drought events due advantageous genomic traits giving a competitive edge when under oxidative stress, (II) the diversity of methanogens and methanotrophs does not change under drought and that not one type of ecotype holds the best ecological niche, and finally, (III) peatlands dominated by sedge species *E. vaginatum* yield the highest fluxes of CH_4 under drought conditions. To be able to predict the effect of anthropogenic climate change, including drought events more accurately on methanogen and methanotroph communities, additional attention should be paid toward the frequency and length of drought events. We observe a highly resilient methanogen community, which surprisingly expanded in relative abundance during drought conditions, but this increase is not reflected in CH_4 emissions presumably due to the even higher increase in methanotrophy. This high relative abundance of both communities indicates that the

severe drought from 2018 did not deteriorate the functional potential of the peatland ecosystem to emit CH_4 to the atmosphere.

Data Availability Statement

The annotated sequence data used for analyzing the functional potential of the microbial community in the study are available at the MG-RAST repository via project ID: 91145 (https://www.mg-rast.org/linkin.cgi?project=mgp91145) with open access to the public. The supplement related to the article is available online at https://doi.org/10.5281/zenodo.8246656.

Acknowledgments

We would like to thank the staff from the Centre for Genomic Research, Liverpool and Roche Diagnostics Scandinavia for probe hybridization and sequencing. Special thanks go to our colleagues, friends, and family for the valuable discussions, and a special thanks to field assistants Oskar Ström and Thomas Golin for working tirelessly during the 2018 heatwave. This study has been made possible by the Swedish Infrastructure for Ecosystem Science (SITES), at the Skogaryd research catchment station and was funded by the Swedish Research Council for Sustainable Development (FORMAS) under the Grant 2016-01462. SITES receives funding through the Swedish Research Council under the Grant 2017-00635. Data handling was enabled by resources in project SNIC 2019/8–365 provided by the Swedish National Infrastructure for Computing (SNIC) at UPPMAX. F-JWP was supported through additional funding from the Research Council of Norway (project no. 323945).

References

Amodeo, C., Sofo, A., Tito, M. T., Scopa, A., Masi, S., Pascale, R., et al. (2018). Environmental factors influencing landfill gas biofiltration: Lab scale study on methanotrophic bacteria growth. *Journal of Environmental Science and Health - Part A: Toxic/Hazardous Substances & Environmental Engineering*, *53*(9), 825–831. https://doi.org/10.1080/10934529.2018.1455342

Anderson, M. J. (2001). A new method for non-parametric multivariate analysis of variance [Software]. Austral Ecology, *26*, 32–46. https://doi.org/10.1046/j.1442-9993.2001.01070.x

Angel, R., Matthies, D., & Conrad, R. (2011). Activation of methanogenesis in Arid biological soil crusts despite the presence of oxygen. *PLoS One*, *6*(5), 1–8. https://doi.org/10.1371/journal.pone.0020453

Bates, D., Mächler, M., Bolker, B., & Walker, S. (2015). Fitting linear mixed-effects models using lme4 [software]. Journal of Statistical Software, *67*, 1–48. https://doi.org/10.18637/jss.v067.i01

Borrel, G., Adam, P. S., & Gribaldo, S. (2016). Methanogenesis and the Wood-Ljungdahl pathway: An ancient, versatile, and fragile association. *Genome Biology and Evolution*, *8*(6), 1706–1711. https://doi.org/10.1093/gbe/evw114

Brandt, F. B., Martinson, G. O., Pommerenke, B., Pump, J., & Conrad, R. (2015). Drying effects on archaeal community composition and methanogenesis in bromeliad tanks. *FEMS Microbiology Ecology*, *91*(2), 1–10. https://doi.org/10.1093/femsec/fiu021

Bräuer, S. L., Basiliko, N., Siljanen, M. P., & Zinder, H. (2020). Methanogenic archaea in peatlands. *FEMS Microbiology Letters*, *367*(20). https://doi.org/10.1093/femsle/fnaa172

Buan, N., Kulkarni, G., & Metcalf, W. (2011). Chapter two - genetic methods for Methanosarcina species. In A. C. Rosenzweig & S. W. Ragsdale (Eds.), *Methods in enzymology* (pp. 23–42). Academic Press. https://doi.org/10.1016/B978-0-12-385112-3.00002-0

Conrad, R., Ji, Y., Noll, M., Klose, M., Claus, P., & Enrich-Prast, A. (2014). Response of the methanogenic microbial communities in Amazonian oxbow lake sediments to desiccation stress. *Environmental Microbiology*, *16*(6), 1682–1694. https://doi.org/10.1111/1462-2920.12267

Dean, J. F., Middelburg, J. J., Röckmann, T., Aerts, R., Blauw, L. G., Egger, M., et al. (2018). Methane Feedbacks to the global climate system in a warmer World. *Reviews of Geophysics*, *56*(1), 207–250. https://doi.org/10.1002/2017RG000559

Dedysh, S. N., & Dunfield, P. F. (2011). Chapter three - facultative and obligate methanotrophs: How to identify and differentiate them. In A. C. Rosenzweig & S. W. Ragsdale (Eds.), *Methods in enzymology* (pp. 31–44). Academic Press. https://doi.org/10.1016/B978-0-12-386905-0.00003-6

Erkel, C., Kube, M., Reinhardt, R., & Liesack, W. (2006). Genome of rice cluster I archaea: The key methane producers in the rice rhizosphere. *Science*, *313*(5785), 370–372. https://doi.org/10.1126/science.1127062

Ernst, C., Kayastha, K., Koch, T., Venceslau, S. S., Pereira, I. A. C., Demmer, U., et al. (2021). Structural and spectroscopic characterization of a HdrA-like subunit from *Hyphomicrobium denitrificans*. *FEBS Journal*, *288*(5), 1664–1678. https://doi.org/10.1111/febs.15505

Fenner, N., & Freeman, C. (2011). Drought-induced carbon loss in peatlands. *Nature Geoscience*, *4*(12), 895–900. https://doi.org/10.1038/ngeo1323

Ferry, J. G. (1999). Enzymology of one-carbon metabolism in methanogenic pathways. *FEMS Microbiology Reviews*, *23*(1), 13–38. https://doi.org/10.1111/j.1574-6976.1999.tb00390.x

Ferry, J. G. (2010). CO in methanogenesis. *Annals of Microbiology*, *60*, 1–12. https://doi.org/10.1007/s13213-009-0008-5

Guerrero-Cruz, S., Vaksmaa, A., Horn, M. A., Niemann, H., Pijuan, M., & Ho, A. (2021). Methanotrophs: Discoveries, environmental relevance, and a perspective on current and future applications. *Frontiers in Microbiology*, *12*. https://doi.org/10.3389/fmicb.2021.678057

Hakobyan, A., & Liesack, W. (2020). Unexpected metabolic versatility among type II methanotrophs in the Alphaproteobacteria. *Biological Chemistry*, *401*(12), 1469–1477. https://doi.org/10.1515/hsz-2020-0200

Ho, A., Lüke, C., & Frenzel, P. (2011). Recovery of methanotrophs from disturbance: Population dynamics, evenness and functioning. *ISME J*, *5*(4), 750–758. https://doi.org/10.1038/ismej.2010.163

Ho, A., Van den Brink, E., Reim, A., Krause, S. M., & Bodelier, P. L. (2015). Recurrence and frequency of disturbance have cumulative effect on methanotrophic activity, abundance, and community structure. *Frontiers in Microbiology*, *6*, 1493. https://doi.org/10.3389/fmicb.2015.01493

IPCC. (2021). *Climate change 2021: The physical science basis. Contribution of working group I to the sixth assessment report of the intergovernmental panel on climate change*. In V. P. Masson-Delmotte, A. Zhai, S. L. Pirani, C. Connors, S. Péan, et al. (Eds.) Cambridge University Press.

Joshi, N. A., & Fass, J. N. (2011). Sickle: A sliding-window, adaptive, quality-based trimming tool for FastQ files (version 1.33). *Software*. Retrieved from https://github.com/najoshi/sickle

Kanehisa, M., Sato, Y., Kawashima, M., Furumichi, M., & Tanabe, M. (2015). KEGG as a reference resource for gene and protein annotation [Database]. *Nucleic Acids Research*, *44*(D1), D457–D462. https://doi.org/10.1093/nar/gkv1070

Keane, B. J., Ineson, P., Vallack, H. W., Blei, E., Bentley, M., Howarth, S., et al. (2018). Greenhouse gas emissions from the energy crop oilseed rape (*Brassica napus*); the role of photosynthetically active radiation in diurnal N_2O flux variation. *GCB Bioenergy*, *10*(5), 306–319. https://doi.org/10.1111/gcbb.12491

Keane, J. B., Toet, S., Ineson, P., Weslien, P., Stockdale, J. E., & Klemedtsson, L. (2021). Carbon dioxide and methane flux response and recovery from drought in a hemiboreal ombrotrophic fen. *Frontiers in Earth Science*, *8*. https://doi.org/10.3389/feart.2020.562401

Kelly, J., Kljun, N., Eklundh, L., Klemedtsson, L., Liljebladh, B., Olsson, P.-O., et al. (2021). Modelling and upscaling ecosystem respiration using thermal cameras and UAVs: Application to a peatland during and after a hot drought. *Agricultural and Forest Meteorology*, *300*, 108330. https://doi.org/10.1016/j.agrformet.2021.108330

Kim, B.-R., Shin, J., Guevarra, R., Lee, J. H., Kim, D. W., Seol, K.-H., et al. (2017). Deciphering diversity indices for a better understanding of microbial communities. *Journal of Microbiology and Biotechnology*, *27*(12), 2089–2093. https://doi.org/10.4014/jmb.1709.09027

Kim, S.-Y., Lee, S.-H., Freeman, C., Fenner, N., & Kang, H. (2008). Comparative analysis of soil microbial communities and their responses to the short-term drought in bog, fen, and riparian wetlands. *Soil Biology and Biochemistry*, *40*(11), 2874–2880. https://doi.org/10.1016/j.soilbio.2008.08.004

Kip, N., Van Winden, J. F., Pan, Y., Bodrossy, L., Reichart, G.-J., Smolders, A. J. P., et al. (2010). Global prevalence of methane oxidation by symbiotic bacteria in peat-moss ecosystems. *Nature Geoscience*, *3*(9), 617–621. https://doi.org/10.1038/ngeo939

Korrensalo, A., Männistö, E., Alekseychik, P., Mammarella, I., Rinne, J., Vesala, T., & Tuittila, E. S. (2018). Small spatial variability in methane emission measured from a wet patterned boreal bog. *Biogeosciences*, *15*(6), 1749–1761. https://doi.org/10.5194/bg-15-1749-2018

Kushwaha, S. K., Manoharan, L., Meerupati, T., Hedlund, K., & Ahren, D. (2015). MetCap: A bioinformatics probe design pipeline for large-scale targeted metagenomics. *BMC Bioinformatics*, *16*(1), 65. https://doi.org/10.1186/s12859-015-0501-8

Liebner, S., Zeyer, J., Wagner, D., Schubert, C., Pfeiffer, E.-M., & Knoblauch, C. (2011). Methane oxidation associated with submerged brown mosses reduces methane emissions from Siberian polygonal tundra. *Journal of Ecology*, *99*(4), 914–922. https://doi.org/10.1111/j.1365-2745.2011.01823.x

Lyu, Z., & Lu, Y. (2018). Metabolic shift at the class level sheds light on adaptation of methanogens to oxidative environments. *ISME J*, *12*(2), 411–423. https://doi.org/10.1038/ismej.2017.173

Ma, K., Conrad, R., & Lu, Y. (2012). Responses of methanogen mcrA genes and their transcripts to an alternate dry/wet cycle of paddy field soil. *Applied and Environmental Microbiology*, *78*(2), 445–454. https://doi.org/10.1128/AEM.06934-11

Manoharan, L., Kushwaha, S. K., Hedlund, K., & Ahren, D. (2015). Captured metagenomics: Large-scale targeting of genes based on 'sequence capture' reveals functional diversity in soils. *DNA Research: An International Journal for Rapid Publication of Reports on Genes and Genomes*, *22*(6), 451–460. https://doi.org/10.1093/dnares/dsv026

Martin, M. (2011). Cutadapt removes adapter sequences from high-throughput sequencing reads [Software]. EMBnet Journal, *17*, 3. https://doi.org/10.14806/ej.17.1.200

McGivern, B. B., Tfaily, M. M., Borton, M. A., Kosina, S. M., Daly, R. A., Nicora, C. D., et al. (2021). Decrypting bacterial polyphenol metabolism in an anoxic wetland soil. *Nature Communications*, *12*(1), 2466. https://doi.org/10.1038/s41467-021-22765-1

Meyer, F., Paarmann, D., D'Souza, M., Olson, R., Glass, E. M., Kubal, M., et al. (2008). The metagenomics RAST server—A public resource for the automatic phylogenetic and functional analysis of metagenomes [software]. BMC Bioinformatics, *9*(1), 386. https://doi.org/10.1186/1471-2105-9-386

Miller, K. E., Lai, C.-T., Dahlgren, R. A., & Lipson, D. A. (2019). Anaerobic methane oxidation in high-Arctic Alaskan peatlands as a significant control on net CH_4 fluxes. *Soil Systems*, *3*, 7. https://doi.org/10.3390/soilsystems3010007

Oksanen, J., Blanchet, F. G., Friendly, M., Kindt, R., Legendre, P., McGlinn, D., et al. (2019). Vegan: Community ecology package. *Software*.

R Core Team. (2022). *R: A language and environment for statistical computing, software*. R-Foundation for Statistical Computing.

Rinne, J., Tuovinen, J.-P., Klemedtsson, L., Aurela, M., Holst, J., Lohila, A., et al. (2020). Effect of the 2018 European drought on methane and carbon dioxide exchange of northern mire ecosystems. *Philosophical Transactions of the Royal Society B: Biological Sciences*, *375*(1810), 20190517. https://doi.org/10.1098/rstb.2019.0517

Saunois, M., Stavert, A. R., Poulter, B., Bousquet, P., Canadell, J. G., Jackson, R. B., et al. (2020). The global methane budget 2000–2017. *Earth System Science Data*, *12*(3), 1561–1623. https://doi.org/10.5194/essd-12-1561-2020

Scheller, S., Goenrich, M., Boecher, R., Thauer, R. K., & Jaun, B. (2010). The key nickel enzyme of methanogenesis catalyses the anaerobic oxidation of methane. *Nature*, *465*(7298), 606–608. https://doi.org/10.1038/nature09015

Sjökvist, E., Abdoush, D., & Axén, J. (2019). Sommaren 2018 - En glimt av framtiden? *SMHI, Klimatologi*, *52*.

Thauer, R. K. (2019). Methyl (Alkyl)-Coenzyme M reductases: Nickel F-430-Containing enzymes involved in anaerobic methane formation and in anaerobic oxidation of methane or of short chain alkanes. *Biochemistry*, *58*(52), 5198–5220. https://doi.org/10.1021/acs.biochem.9b00164

Thauer, R. K., Kaster, A.-K., Seedorf, H., Buckel, W., & Hedderich, R. (2008). Methanogenic archaea: Ecologically relevant differences in energy conservation. *Nature Reviews Microbiology*, *6*(8), 579–591. https://doi.org/10.1038/nrmicro1931

Van Hulzen, J. B., Segers, R., Van Bodegom, P. M., & Leffelaar, P. A. (1999). Temperature effects on soil methane production: An explanation for observed variability. *Soil Biology and Biochemistry*, *31*(14), 1919–1929. https://doi.org/10.1016/S0038-0717(99)00109-1

Vicente-Serrano, S. M., Beguería, S., & López-Moreno, J. I. (2010). A multiscalar drought index sensitive to global warming: The standardized precipitation evapotranspiration index. *Journal of Climate*, *23*(7), 1696–1718. https://doi.org/10.1175/2009jcli2909.1

Villanueva, R. A. M., & Chen, Z. J. (2019). ggplot2: Elegant graphics for data analysis (software). *Measurement: Interdisciplinary Research and Perspectives*, *17*, 160–167. https://doi.org/10.1080/15366367.2019.1565254

Wallin, M. B., Weyhenmeyer, G. A., Bastviken, D., Chmiel, H. E., Peter, S., Sobek, S., & Klemedtsson, L. (2015). Temporal control on concentration, character, and export of dissolved organic carbon in two hemiboreal headwater streams draining contrasting catchments. *Journal of Geophysical Research: Biogeosciences*, *120*(5), 832–846. https://doi.org/10.1002/2014JG002814

Weiss, S., Xu, Z. Z., Peddada, S., Amir, A., Bittinger, K., Gonzalez, A., et al. (2017). Normalization and microbial differential abundance strategies depend upon data characteristics. *Microbiome*, *5*(1), 27. https://doi.org/10.1186/s40168-017-0237-y

Wendlandt, K.-D., Stottmeister, U., Helm, J., Soltmann, B., Jechorek, M., & Beck, M. (2010). The potential of methane-oxidizing bacteria for applications in environmental biotechnology. *Engineering in Life Sciences*, *10*, 87–NA. https://doi.org/10.1002/elsc.200900093

White, J. D., Ström, L., Lehsten, V., Rinne, J., & Ahrén, D. (2022). Genetic functional potential displays minor importance in explaining spatial variability of methane fluxes within a *Eriophorum vaginatum* dominated Swedish peatland. *Biogeosciences Discussions*, 1–38. https://doi.org/10.5194/bg-2021-353

Wilmoth, J. L., Schaefer, J. K., Schlesinger, D. R., Roth, S. W., Hatcher, P. G., Shoemaker, J. K., & Zhang, X. (2021). The role of oxygen in stimulating methane production in wetlands. *Global Change Biology*, *27*(22), 5831–5847. https://doi.org/10.1111/gcb.15831

Yu, Z. C. (2012). Northern peatland carbon stocks and dynamics: A review. *Biogeosciences*, *9*(10), 4071–4085. https://doi.org/10.5194/bg-9-4071-2012

Yuan, Y., Conrad, R., & Lu, Y. (2009). Responses of methanogenic archaeal community to oxygen exposure in rice field soil. *Environmental Microbiology Reports*, *1*(5), 347–354. https://doi.org/10.1111/j.1758-2229.2009.00036.x

Zhang, W., Kang, X., Kang, E., Audet, J., Davidson, T. A., Zhang, X., et al. (2022). Soil water content, carbon, and nitrogen determine the abundances of methanogens, methanotrophs, and methane emission in the Zoige alpine wetland. *Journal of Soils and Sediments*, *22*(2), 470–481. https://doi.org/10.1007/s11368-021-03043-5

Zhong, Q., Chen, H., Liu, L., He, Y., Zhu, D., Jiang, L., et al. (2017). Water table drawdown shapes the depth-dependent variations in prokaryotic diversity and structure in Zoige peatlands. *FEMS Microbiology Ecology*, *93*(6). https://doi.org/10.1093/femsec/fix049

References From the Supporting Information

Keegan, K. P., Trimble, W. L., Wilkening, J., Wilke, A., Harrison, T., D'Souza, M., & Meyer, F. (2012). A platform-independent method for detecting errors in metagenomic sequencing data: DRISEE. *PLoS Computational Biology*, *8*(6), e1002541. https://doi.org/10.1371/journal.pcbi.1002541

Langmead, B., Trapnell, C., Pop, M., & Salzberg, S. L. (2009). Ultrafast and memory-efficient alignment of short DNA sequences to the human genome. *Genome Biology*, *10*(3), R25. https://doi.org/10.1186/gb-2009-10-3-r25

Edgar, R. C. (2010). Search and clustering orders of magnitude faster than BLAST. *Bioinformatics*, *26*(19), 2460–2461. https://doi.org/10.1093/bioinformatics/btq461

Caporaso, J. G., Kuczynski, J., Stombaugh, J., Bittinger, K., Bushman, F. D., Costello, E. K., et al. (2010). QIIME allows analysis of high-throughput community sequencing data. *Nature Methods*, *7*(5), 335–336. https://doi.org/10.1038/nmeth.f.303